

Characterization of Thin Polymer Films by X-ray Reflectometry with Synchrotron Radiation

Keitaro Kago,^a Hitoshi Endo,^a Hideki Matsuoka,^a Hitoshi Yamaoka,^{a*} Nozomu Hamaya,^b Masahiko Tanaka^c and Takeharu Mori^c

^aDepartment of Polymer Chemistry, Kyoto University, Kyoto 606-8501, Japan, ^bDepartment of Physics, Ochanomizu University, Tokyo 112-8610, Japan, and ^cPhoton Factory, National Laboratory for High Energy Physics, Oho, Tsukuba 305-0801, Japan.
E-mail: yamaoka@star.polym.kyoto-u.ac.jp

(Received 20 July 1997; accepted 11 May 1998)

X-ray reflectivity (XR) measurements with a synchrotron radiation source were carried out for thin polymer films on a glass plate. From the XR data, the film thickness and surface and interface roughnesses could be determined. In addition, the appropriate conditions and precision for measurements were also discussed. Kiessig fringes were observed clearly for specular XR measurements of poly(methylmethacrylate) thin film. Analysis of the XR data allowed the determination of the film thickness very precisely. By a curve-fitting procedure of the XR profile, the film-surface roughness and film-substrate interface roughnesses were determined. A Fourier transform of the XR data was performed as an alternative method of evaluating the film thickness. The values for the film thickness obtained by the curve-fitting procedure and Fourier-transform procedure were slightly different from each other. One possibility for the cause of this difference may be an integral error and/or cut-off effect in the Fourier-transform procedure. The XR technique with synchrotron radiation is a very powerful tool for structural characterization of thin polymer films.

Keywords: X-ray reflectivity; thin polymer films; Kiessig fringes; surface roughness; Fourier transform.

1. Introduction

The refractive index of X-rays is slightly less than unity for most substances. When the glancing angle of the incident X-rays into a plane surface is below the critical angle of the substance, total reflection occurs, although the critical angle is very small, $<1^\circ$. In this case, the evanescent wave is generated into the substrate with a penetration depth of $\sim 10 \text{ \AA}$ ($1 \times 10^{-3} \text{ \mu m}$). On the other hand, when the glancing angle of the incident X-rays is above the critical angle, part of the X-ray is reflected and part passes into the substance with a certain refracted angle and can penetrate the substance down to $\sim 100 \text{ \mu m}$, much deeper than the evanescent wave. If the substance has a second interface, such as a thin polymer film on the substrate, the X-rays reflected at the polymer surface and the polymer-substrate interface produce an interference effect; the XR profile shows an oscillation behaviour known as Kiessig fringes (Kiessig, 1931). Kiessig measured the X-ray reflectivity for nickel films by photometry and observed interference fringes. The period of the oscillation reflects the film thickness, and the decay of the oscillation is related to the surface and interface roughnesses, as will be described later in detail.

The importance of surface and interface analysis is increasing. The knowledge obtained for the microstructure

near the surface and interface and for thin films has played an important role in industrial applications, chemical engineering *etc.* This information can be obtained by XR measurements since it provides an electron density profile normal to the surface. XR is an adequate method of analyzing surface and interfacial structure. The advantages of XR measurement are (i) the resolution is very high; since the wavelength of X-rays is a few angstroms, the resolution is of the order of angstroms while conventional techniques of analyzing the surface and interfacial structure of polymers were of the order of nanometres (Stamm, 1992); (ii) measurement is non-destructive; (iii) not only the surface structure, but also the electron density profile

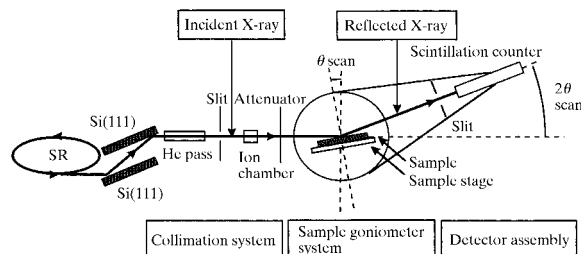


Figure 1
Apparatus for XR measurements using synchrotron radiation (SR) at the Photon Factory.

normal to the surface from the vicinity of the surface to deeper parts of the substance, can be analyzed (specular reflection measurement). The application of this technique to thin polymer films on solid substrates allows the determination of various parameters; the refractive index of the polymer, film thickness and surface and film–substrate interface roughnesses can be determined (Foster *et al.*, 1990; Mayes *et al.*, 1994). The structures of not only polymer films but also other kinds of films, such as liquid films on solid substrates (Pershan, 1994) and SiO₂ ultrathin films on Si (Awaji *et al.*, 1996), are analyzed by XR using synchrotron radiation.

Suppose that a system consists of three stratified homogeneous media, *i.e.* air/film/substrate. Kiessig fringes should be observed when the glancing angle of incident X-rays is above the critical angle of the film. In this case, Kiessig fringes are a result of the interference between the reflected X-rays at the film surface and film–substrate interface. The positions of the maxima and minima of the fringe are related to the refractive index and the film thickness. Parratt (1954) analyzed the XR specular curve in the region of total reflection and showed that X-ray reflectivity was expressed using the recursive equation of the function of the Fresnel coefficient for reflection and reflection coefficient for each interface. Sinha *et al.* (1988) calculated the effect of surface and interface roughnesses based on the distorted-wave Born approximation.

In the present paper, we will discuss the application of the XR technique using synchrotron radiation to thin polymer films and of the Fourier-transform procedure to the XR data. Synchrotron radiation was used to provide the strong tunable monochromatic X-rays with sufficiently high flux density. These features made it possible to measure the X-ray reflectivity for thin polymer films.

2. Experimental

2.1. Apparatus

The XR experiments with synchrotron radiation were performed at beamline BL-3A at the Photon Factory, National Laboratory for High Energy Physics, Tsukuba, Japan (Kago *et al.*, 1995, 1996). This beamline was originally constructed as a four-circle goniometer but we have modified this to a reflectometer. The apparatus consisted of a collimation system, sample goniometer system and detector assembly. The outline of the apparatus is schematically shown in Fig. 1. The incident X-ray beam from the synchrotron radiation ring is monochromized by a double-crystal monochromator consisting of a pair of parallel Si(111) crystals. The wavelength of incident X-rays was adjusted to be 1.54 Å by this monochromator. Incident X-rays passed through an He guide tube; after that, X-rays travelled in air. The intensity of the incident X-rays was monitored with an ion chamber. The beam was then collimated by the slit whose gap was 0.05 mm in height and 2 mm in width. When the measurements were performed at low glancing angles, a 0.5 mm aluminium plate was

attached as an attenuator at the front of the sample in order to protect the scintillation counter from radiation damage by the strong direct beam or totally reflected beam.

The sample goniometer system consisted of a goniometer and sample stage. Measurements were performed so that the scattering angle 2θ was a double portion of the incident angle θ ; in other words, the reflectivity was measured for the reflection angle being the same as the incident angle. This is known as specular reflection. The typical angular step was 0.01° in 2θ . The sample stage could be moved vertically. Optical alignment was performed by moving the sample stage so that the intensity of the totally reflected X-rays became strongest when the incident angle was equal to the critical angle of the substrate.

The reflected X-rays passed through a slit whose gap was the same as that for the incident X-rays. This slit was used to reduce the effect of diffuse scattering at the film surface. The intensity of the reflected X-rays was detected with a scintillation counter. The intensity data of incident and reflected X-rays were recorded by computer.

2.2. Sample preparation

The materials used here were poly(methylmethacrylate) (PMMA, extra pure reagent; Nacalai tesque Inc., Kyoto, Japan) and polystyrene (PS, reagent; Nacalai tesque Inc., Kyoto, Japan). The weight average molecular weights of PMMA and PS were about 700000 and 100000, respectively. Thin polymer films were prepared by the spin-coating method. This method can provide us with thin smooth homogeneous polymer films of large area on solid substrates. Spinning began after adding drops of polymer solutions on Pyrex glass plates. The diameter of the glass plates was 5.5 cm. For preparing PMMA and PS films, 0.25 wt% PMMA/acetic acid solution and 0.5 wt% PS/cyclohexane solution were added dropwise, respectively. After the first slow spin of rotation of the plates at 100 r.p.m. for 1 s, the second spin was performed subsequently at 7000 r.p.m. for 99 s. Films were dried *in vacuo* for 1 h.

2.3. Data analysis

XR is a function of the refractive indices of the substances. The complex refractive index of a substance for X-rays is written as (Rieutord *et al.*, 1987)

$$n = 1 - \delta - i\beta, \quad (1)$$

where

$$\delta = (\lambda^2/2\pi)r_e(f + \Delta f')\rho/M, \quad (2)$$

$$\beta = (\lambda^2/2\pi)r_e(\Delta f'')\rho/M, \quad (3)$$

r_e is the classical electron radius, $f + \Delta f' + i\Delta f''$ is the complex atomic scattering factor (Cromer & Liberman, 1974), ρ is the density and M is the atomic mass. The refractive index is the unique parameter for identifying the substance.

The general expression for XR, R , for an N -layered film on a substrate, which was presented by Parratt (1954), is

$$R = I_R/I_0 = |R_{1,2}|^2, \quad (4)$$

where

$$R_{n-1,n} = a_{n-1}^4 [(R_{n,n+1} + F_{n-1,n}) / (R_{n,n+1} F_{n-1,n} + 1)], \quad (5)$$

$$a_n = \exp[-i(\pi/\lambda) f_n d_n], \quad (6)$$

$$f_n = (\theta^2 - 2\delta_n - 2i\beta_n)^{1/2}, \quad (7)$$

$$F_{n-1,n} = (f_{n-1} - f_n) / (f_{n-1} + f_n), \quad (8)$$

and I_0 is the incident intensity, I_R is the reflected intensity, $n_n = 1 - \delta_n - i\beta_n$ is the complex refractive index, d_n is the layer thickness of the n th layer ($2 \leq n \leq N + 2$, layer 1 corresponds to air and layer $N + 2$ corresponds to the substrate), $F_{n-1,n}$ is the Fresnel coefficient for reflection and $R_{n-1,n}$ is the reflection coefficient for the $(n - 1)$ th and n th layer interface. For a rough surface and/or interface, the Fresnel coefficient for reflection is written as

$$F_{n-1,n} = \frac{f_{n-1} - f_n}{f_{n-1} + f_n} \exp(-8\pi f_{n-1} f_n \sigma_n^2 / \lambda^2), \quad (9)$$

where σ_n is the surface or interfacial roughness.

Calculation and analysis of the X-ray reflectivity was performed using the scientific software *MUREX* (multiple reflection of X-rays) (Sakurai, 1995). It is not only used for X-ray reflectivity but also for fluorescence intensity from multilayered thin films in grazing-incidence/exit X-ray experiments.

An attempt to determine the film thickness directly from the oscillation period in the XR profile has been made. However, this is only possible in the case of a single film layer on a substrate. Sakurai & Iida (1992) and Sakurai (1993) pointed out that the reflectivity was expressed in terms of the cosine function of $4\pi d(\theta^2 - \theta_c^2)^{1/2}/\lambda$ (θ and θ_c are the glancing and critical angles for the film, respectively, λ is the wavelength of the incident X-rays and d is the film thickness) for a single film layer, and showed that the film thickness was determined by a Fourier-transform procedure

of the oscillating component of the XR data. It allowed the determination of not only the total film thickness but also each layer thickness of multilayered films. That is, after the reflectivity was expressed as a function of $(\theta^2 - \theta_{cj}^2)^{1/2}/\lambda$ (θ_{cj} is the critical angle for j th film), a Fourier transform was performed and each layer thickness could be determined. Because the roughness did not affect the period of oscillation, the film thickness could be determined independently of the surface and interface roughnesses. It is the advantage of the Fourier-transform procedure that each layer thickness of a multilayered film can be determined and that roughnesses do not affect the analysis.

3. Results and discussion

Fig. 2 shows the XR curve for PMMA thin film on a glass plate. Reflectivity down to 10^{-7} could be detected. Such a high order of reflectivity could be achieved not only by using synchrotron radiation but also by the reduction of the background intensity using a lead plate surrounding the scintillation counter; the background intensity was lowered to approximately 0.1 counts s^{-1} . In the scattering vector [\mathbf{q} ($= 4\pi \sin\theta/\lambda$)] range from 0 to 0.13 \AA^{-1} , the measurements were performed with an attenuator in order to protect the scintillation counter from direct incident X-rays, while in the large- \mathbf{q} range, above 0.13 \AA^{-1} , the measurements were performed without an attenuator. The angular step was 0.02° in 2θ . The accumulation time for each angle was 20 s for the measurements at lower angles and 10 s for wider angles. Since the diameter of the glass plates was 5.5 cm and the height of the incident beam was 0.05 mm, as mentioned previously, part of the incident beam did not hit the sample surface due to a larger area of projection than that of the sample in the very small \mathbf{q} range below 0.007 \AA^{-1} or 0.1° in 2θ . Therefore, in this range, the measured reflectivity is apparently lower.

Theoretically, the reflectivity has to be almost unity in the \mathbf{q} range below the critical angle since total reflection should occur. However, the experimental data show lower reflectivity. This may be due to the glass surface not being

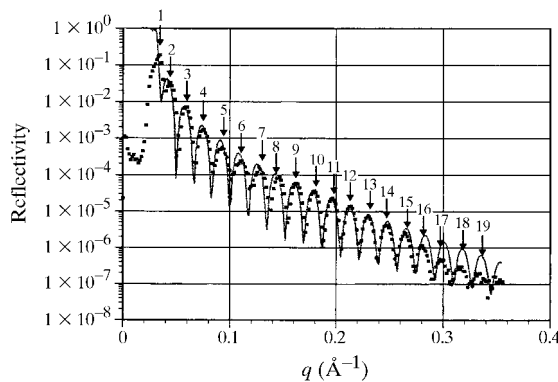


Figure 2
XR curve for PMMA thin film on a glass plate. The solid line is the best fit to the experimental data (dots).

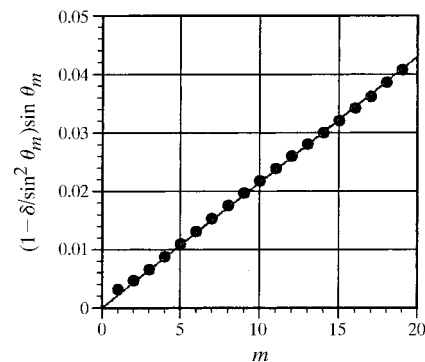


Figure 3
Relation between the position of the maxima of the Kiessig fringes, θ_m , and the interference order m for PMMA thin film on a glass plate. The slope of the straight line corresponds to $\lambda/2d$.

perfectly flat and the sample alignment not being exactly precise.

In Fig. 2, Kiessig fringes were clearly observed above the critical angle; up to the 19th maxima of the fringe was detected. This means that thin PMMA film on a glass plate is almost homogeneous in density and its thickness is well controlled. The position of the maxima of the fringe, θ_m , is given by the equation (Compton, 1923)

$$(1 - \delta/\sin^2 \theta_m) \sin \theta_m = m\lambda/2d, \quad (10)$$

where m is an interference order. Equation (10) means that the $(1 - \delta/\sin^2 \theta_m) \sin \theta_m$ versus m plot should be a straight line with the slope equal to $\lambda/2d$. Such a plot is shown in Fig. 3. The linearity of the plot is satisfactory. From the slope of this straight line, the film thickness d was determined to be $356 \pm 2 \text{ \AA}$.

Curve fitting was carried out for the XR data above the critical angle. Surface and interface roughnesses are determined by a model fit to the experimental data. This was performed by changing the surface and interface roughnesses with a fixed value of refractive index. Roughness has the same effect on reflectivity as a continuous change in refractive index, *i.e.* electron density profile at the interface. A result of the fitting is shown in Fig. 2 as a solid line. An excellent agreement was observed using a model with a homogeneous layer of the film and an error function type of profile for the density change at the interface. The surface and film-substrate interface roughnesses were determined to be 4 and 5 \AA , respectively.

A Fourier transform of the XR data was carried out as an alternative method for evaluating film thickness. First, the data obtained was smoothed so that the oscillating component was not observed. Then, the original data was divided by the smoothed data. As a result, the cosine oscillating component was extracted. The data were plotted as a function of $(\theta^2 - \theta_c^2)^{1/2}/\lambda$ followed by Fourier transform. Fig. 4 shows the result of the Fourier transform. In Fig. 4, the abscissa is the film thickness and the ordinate is the magnitude of the Fourier transform which corresponds to the probability of existence of that thickness. A single peak was observed in Fourier space although very small

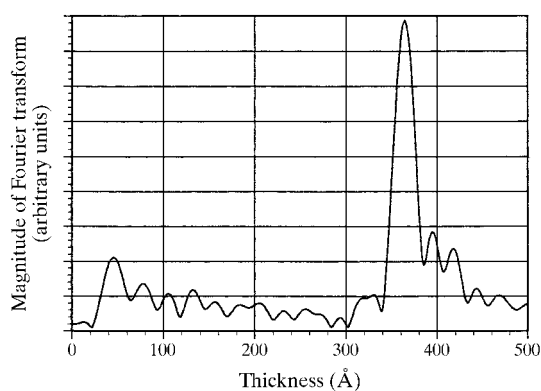


Figure 4 Magnitude of the Fourier transform of the oscillating component extracted from XR data for PMMA thin film.

Fourier ripples are also observed. The peak position corresponds to the frequency of oscillation, *i.e.* the film thickness [recall that the reflectivity was a function of $\cos[4\pi d(\theta^2 - \theta_c^2)^{1/2}/\lambda]$]. By this procedure, the film thickness was determined to be 364 \AA , which is slightly different from the value obtained by the curve-fitting procedure ($356 \pm 2 \text{ \AA}$).

One possibility for the reason of this difference may be an integral error and/or cut-off effect in the Fourier-transform procedure. As is seen in Fig. 2, the oscillating behaviour of the XR curve has not yet decayed in the angle range measured, which may cause at least a cut-off effect (termination effect) in the Fourier-transform procedure. Hence, the Fourier-transform procedure is useful for the data whose oscillating component converged and in which sufficient numbers of fringes were observed.

Fig. 5 shows the XR curve for PS thin film. In the scattering vector (\mathbf{q}) range from 0 to 0.13 \AA^{-1} , the measurement was performed with an attenuator, while in the \mathbf{q} range above 0.13 \AA^{-1} it was performed without an attenuator. The angular step was 0.01° and 0.02° in 2θ and the accumulation time was 40 s and 10 s for lower and wider angles, respectively. Clear Kiessig fringes are also observed in this case. At least nine maxima can be seen. Also for this data, a curve-fitting procedure was performed. The best-fit curve is shown in Fig. 5 as a solid line. The agreement is satisfactory and the film thickness was determined to be $203 \pm 3 \text{ \AA}$ and the surface and film-substrate interface roughnesses to be 8 and 5 \AA , respectively. By Fourier-transform procedure, the film thickness was determined to be 203 \AA , which agrees well with the value obtained by the curve-fitting procedure. This is due to the fact that the Fourier transform was carried out for the data whose oscillating component converged. The oscillating behaviour for PS film in Fig. 5 is almost converged, especially compared with that for PMMA film in Fig. 2. In the case of PMMA, the deviation of the thickness calculated by the Fourier-transform procedure (364 \AA) from that determined by the curve-fitting procedure (356 \AA) was about 2%. On the other hand, in the case of PS, no apparent deviation was observed. It should involve a

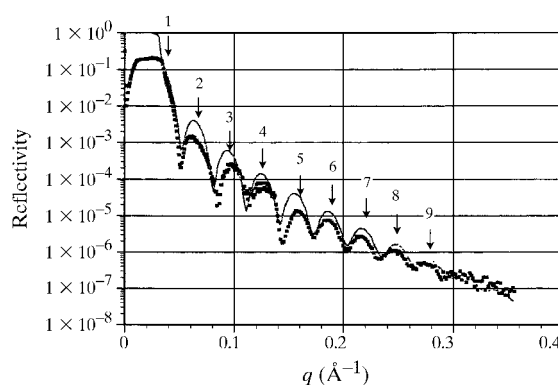


Figure 5 XR curve for PS thin film on a glass plate. The solid line is the best fit to the experimental data (dots).

smaller cut-off effect in integration calculation in the Fourier-transform procedure and result in agreement of the value obtained by the Fourier-transform procedure with that obtained by the curve-fitting procedure. It was quantitatively confirmed that the oscillating component should converge to the extent of the data shown in Fig. 5 when the Fourier transform was performed to determine the film thickness.

4. Conclusions

Although the XR apparatus is a modification of a four-circle goniometer, we have succeeded in obtaining high-quality XR data with high resolution and wide dynamic range for intensity detection (down to 10^{-7} of reflectivity). It is confirmed that the XR technique is a very powerful and sensitive method for investigating the characteristics of thin polymer films; clear Kiessig fringes were observed both for PMMA and PS thin films on a glass plate. The resolution of the XR measurement for the determination of film thickness and surface and interface roughnesses is of the order of angstroms, which exceeds that of the other techniques.

Non-destructive observations can be carried out for XR measurements. This is a great advantage of the XR technique; specific sample treatment such as cutting (IR densitometry), staining (transmission electron microscopy) and the deposition of a conductive metal film on the top (scanning electron microscopy) is not necessary. Moreover, XR measurements can be performed in air or under low-vacuum conditions. Therefore, more direct information can be obtained and more detailed analysis becomes possible for the surface and interfacial structure by XR. In this study, we have examined one uniform thin layer of a polymer on a substrate. The next target is a multilayered film, a composite material. XR results on such a system will be described in a forthcoming paper. In addition, XR

should be applied to a polymer monolayer at the liquid-vapour interface. Such experiments are already under way in our laboratory (Kago *et al.*, 1998; Yamaoka *et al.*, 1998).

References

- Awaji, N., Ohkubo, S., Nakanishi, T., Sugita, Y., Takasaki, K. & Komiya, S. (1996). *Jpn. J. Appl. Phys.* **35**, L67–70.
- Compton, A. H. (1923). *Philos. Mag.* **45**, 1121–1131.
- Cromer, D. T. & Liberman, D. (1974). *International Tables for X-ray Crystallography*, Vol. 4, edited by J. A. Ibers & W. C. Hamilton, pp. 148–151. Birmingham: Kynock Press.
- Foster, M., Stamm, M., Reiter, G. & Huettenbach, S. (1990). *Vacuum*, **41**, 1441–1444.
- Kago, K., Endo, H., Matsuoka, H., Yamaoka, H. & Hamaya, N. (1996). *Photon Factory Activity Report 14*, p. 26. Photon Factory, Oho, Ibaraki 305, Japan.
- Kago, K., Matsuoka, H., Endo, H., Eckelt, J. & Yamaoka, H. (1998). *Supramol. Sci.* In the press.
- Kago, K., Tanimoto, S., Matsuoka, H., Yamaoka, H. & Hamaya, N. (1995). *Photon Factory Activity Report 13*, p. 27. Photon Factory, Oho, Ibaraki 305, Japan.
- Kiessig, H. (1931a). *Ann. Phys.* **10**, 715–768.
- Kiessig, H. (1931b). *Ann. Phys.* **10**, 769–788.
- Mayes, A. M., Russell, T. P., Bassereau, P., Baker, S. M. & Smith, G. S. (1994). *Macromolecules*, **27**, 749–755.
- Parratt, L. G. (1954). *Phys. Rev.* **95**, 359–369.
- Pershan, P. S. (1994). *J. Phys. Condens. Matter*, **6**, A37–50.
- Rieutord, F., Benattar, J. J., Bosio, L., Robin, P., Blot, C. & De Kouchkovsky, R. (1987). *J. Phys.* **48**, 679–687.
- Sakurai, K. (1993). *Bull. Jpn. Inst. Met.* **32**, 323–330.
- Sakurai, K. (1995). *MUREX118. Program for Calculation/Analysis of X-ray Reflectivity, Fluorescence Intensity from Multilayered Thin Films in Grazing-Incidence/Exit X-ray Experiments*. National Research Institute for Metals, Tsukuba, Japan.
- Sakurai, K. & Iida, A. (1992). *Jpn. J. Appl. Phys.* **31**, L113–115.
- Sinha, S. K., Sirota, E. B., Garoff, S. & Stanley, H. B. (1988). *Phys. Rev. B*, **38**, 2297–2311.
- Stamm, M. (1992). *Adv. Polym. Sci.* **100**, 357–400.
- Yamaoka, H., Matsuoka, H., Eckelt, J., Kago, K. & Endo, H. (1998). Submitted.